Three-dimensional mapping of optical near field with scattering SNOM

Yan Li, Nan Zhou, Arvind Raman, and Xianfan Xu[*]

School of Mechanical Engineering and Birck Nanotechnology Center, Purdue University, West Lafayette, Indiana 47907, USA
[*]*xxu@ecn.purdue.edu*

Abstract: Scattering-type scanning near-field optical microscopy (s-SNOM) is applied to investigate three-dimensional optical near field distribution, including both amplitude and phase information. A method analogous to the force volume mode of the atomic force microscopy (AFM) technique is adapted for the measurement. The results show high lateral resolution of tens of nanometers, and even higher vertical resolution of only a few nanometers. The experiment results provide a straightforward illustration of the optical near fields in the space above the sample surface. Numerical computations support the experimental data. The ability to map the 3D optical near filed helps to reveal the factors that influence the performance of the designed near-field structures.

References and links

1. A. Campion and P. Kambhampati, "Surface-enhanced Raman scattering," Chem. Soc. Rev. **27**(4), 241–250 (1998).
2. S. M. Uppuluri, E. C. Kinzel, Y. Li, and X. Xu, "Parallel optical nanolithography using nanoscale bowtie aperture array," Opt. Express **18**(7), 7369–7375 (2010).
3. L. Pan, Y. Park, Y. Xiong, E. Ulin-Avila, Y. Wang, L. Zeng, S. Xiong, J. Rho, C. Sun, D. B. Bogy, and X. Zhang, "Maskless plasmonic lithography at 22 nm resolution," Sci. Rep. **1**, 175 (2011).
4. B. J. Roxworthy, K. D. Ko, A. Kumar, K. H. Fung, E. K. C. Chow, G. L. Liu, N. X. Fang, and K. C. Toussaint, Jr., "Application of plasmonic bowtie nanoantenna arrays for optical trapping, stacking, and sorting," Nano Lett. **12**(2), 796–801 (2012).
5. N. Yu, E. Cubukcu, L. Diehl, D. Bour, S. Corzine, J. Zhu, G. Höfler, K. B. Crozier, and F. Capasso, "Bowtie plasmonic quantum cascade laser antenna," Opt. Express **15**(20), 13272–13281 (2007).
6. T. Ichimura, N. Hayazawa, M. Hashimoto, Y. Inouye, and S. Kawata, "Tip-enhanced coherent anti-stokes Raman scattering for vibrational nanoimaging," Phys. Rev. Lett. **92**(22), 220801 (2004).
7. G. Lérondel, S. Kostcheev, and J. Plain, "Nanofabrication for plasmonics," in Plasmonics, S. Enoch and N. Bonod, eds., (Springer, 2012).
8. E. X. Jin and X. Xu, "Enhanced optical near field from a bowtie aperture," Appl. Phys. Lett. **88**(15), 153110 (2006).
9. R. Guo, E. C. Kinzel, Y. Li, S. M. Uppuluri, A. Raman, and X. Xu, "Three-dimensional mapping of optical near field of a nanoscale bowtie antenna," Opt. Express **18**(5), 4961–4971 (2010).
10. F. Keilmann and R. Hillenbrand, "Near-field microscopy by elastic light scattering from a tip," Philos. Trans. A Math. **362**(1817), 787–805 (2004).
11. M. Schnell, A. Garcia-Etxarri, A. J. Huber, K. B. Crozier, A. Borisov, J. Aizpurua, and R. Hillenbrand, "Amplitude- and phase-resolved near-field mapping of infrared antenna modes by transmission-mode scattering-type near-field microscopy," J. Phys. Chem. C **114**(16), 7341–7345 (2010).
12. M. Rang, A. C. Jones, F. Zhou, Z. Y. Li, B. J. Wiley, Y. Xia, and M. B. Raschke, "Optical near-field mapping of plasmonic nanoprisms," Nano Lett. **8**(10), 3357–3363 (2008).
13. M. Schnell, A. Garcia-Etxarri, J. Alkorta, J. Aizpurua, and R. Hillenbrand, "Phase-resolved mapping of the near-field vector and polarization state in nanoscale antenna gaps," Nano Lett. **10**(9), 3524–3528 (2010).
14. R. Hillenbrand and F. Keilmann, "Complex optical constants on a subwavelength scale," Phys. Rev. Lett. **85**(14), 3029–3032 (2000).
15. R. L. Olmon, M. Rang, P. M. Krenz, B. A. Lail, L. V. Saraf, G. D. Boreman, and M. B. Raschke, "Determination of electric-field, magnetic-field, and electric-current distributions of infrared optical antennas: a near-field optical vector network analyzer," Phys. Rev. Lett. **105**(16), 167403 (2010).
16. H. J. Butt, B. Cappella, and M. Kappl, "Force measurements with the atomic force microscope: technique, interpretation and applications," Surf. Sci. Rep. **59**(1-6), 1–152 (2005).

17. N. Zhou, Y. Li, and X. Xu, "Resolving near-field from high order signals of scattering near-field scanning optical microscopy," Opt. Express **22**(15), 18715–18723 (2014).
18. Y. Li, N. Zhou, E. C. Kinzel, X. Ren, and X. Xu, "The origin of interferometric effect involving surface plasmon polariton in scattering near-field scanning optical microscopy," Opt. Express **22**(3), 2965–2972 (2014).
19. N. Ocelic, A. Huber, and R. Hillenbrand, "Pseudoheterodyne detection for background-free near-field spectroscopy," Appl. Phys. Lett. **89**(10), 101124 (2006).
20. S. Hu and A. Raman, "Inverting amplitude and phase to reconstruct tip-sample interaction forces in tapping mode atomic force microscopy," Nanotechnology **19**(37), 375704 (2008).
21. R. García and A. San Paulo, "Attractive and repulsive tip-sample interaction regimes in tapping-mode atomic force microscopy," Phys. Rev. B **60**(7), 4961–4967 (1999).
22. E. X. Jin and X. Xu, "Obtaining super resolution light spot using surface plasmon assisted sharp ridge nanoaperture," Appl. Phys. Lett. **86**(11), 111106 (2005).
23. E. X. Jin and X. Xu, "Plasmonic effects in near-field optical transmission enhancement through a single bowtie-shaped aperture," Appl. Phys. B **84**(1-2), 3–9 (2006).
24. H. U. Yang, R. L. Olmon, K. S. Deryckx, X. G. Xu, H. A. Bechtel, Y. Xu, B. A. Lail, and M. B. Raschke, "Accessing the optical magnetic near-field through Babinet's principle," ACS Photonics **1**(9), 894–899 (2014).
25. Y. Oshikane, T. Kataoka, M. Okuda, S. Hara, H. Inoue, and M. Nakano, "Observation of nanostructure by scanning near-field optical microscope with small sphere probe," Sci. Technol. Adv. Mater. **8**(3), 181–185 (2007).

1. Introduction

Plasmonic structures have drawn great attentions because of their abilities to efficiently increase the light-matter interaction, and enhance and confine the electromagnetic fields at the nanometer scale. These capabilities have led to a wide range of applications, such as surface enhanced Raman spectroscopy [1], high resolution optical lithography [2,3], plasmonic optical tweezers [4], nanophotonic devices [5], and high resolution optical spectroscopy [6]. For a desired functionality, the design of a plasmonic structure is usually determined through numerical simulations of electromagnetic fields. While this process could qualitatively define the response of the plasmonic structure, the performance of the structure also heavily relies on the fabrication techniques and the operation conditions of the device. For plasmonic structures, the nanometric dimensions, especially for features like nanoscale gaps and sharp structures, are critical to the characteristics of the structures' optical responses. Their fabrication is usually hindered by the achievable resolution limited by current techniques [7]. Thus an experimental investigation of the optical near field distribution can provide valuable information on the validation of the design and evaluation of the performance of the devices.

There have been a significant amount of efforts dedicated to visualizing the optical near field distribution of plasmonic structures, especially by applying scanning near-field optical microscopy (SNOM). For example, with aperture type SNOM, the optical near field distribution of bowtie apertures has been mapped in both two and three dimensions [8,9] at visible wavelength. The scattering-type SNOM (s-SNOM) can achieve higher resolution, on the order of 10 nm, and acquire both amplitude and phase information simultaneously [10]. Using s-SNOM, the amplitude and phase of optical near field in the horizontal plane have been obtained for several nano-structures in the long wavelength infrared range, such as rods, disks, triangle antennas and bowtie apertures [11–13]. Some measurements in the vertical plane were also presented in a few studies [14,15]. Most of the previous researches were conducted in two-dimensional plane mapping or one-dimensional line scanning, especially for the case of s-SNOM.

In this work, three-dimensional mapping of the amplitude and phase of optical near field is conducted using s-SNOM. With the applied method, it is possible to construct the full three-dimensional distribution of the optical near fields. The method has the potential of providing a full characterization of the complex vector fields, and thus a direct evaluation of the functionality and performance of the designed structures.

2. Experimental

The method we use for three-dimensional mapping is based on the s-SNOM technique. The s-SNOM technique utilizes the high spatial resolution of the scanning probe microscopy (SPM) and the optical antenna effect of a nanoscale sharp tip to characterize optical phenomena at

nanoscale. S-SNOM measurements are generally performed in the form of two-dimensional plane scanning or one-dimensional tip-sample distance curve measurement. To achieve three-dimensional mapping, the force volume method in Atomic Force Microscopy (AFM) technique is adapted in this work. In AFM, the force volume method is used to obtain force-distance curves with the scan of the sample surface, producing a two-dimensional array of line curves in the vertical Z direction [16]. When applied this method in s-SNOM, the fact that the tip moves above the sample surface enables the collection of the three-dimensional optical field information. To collect the optical near field information, the s-SNOM tip can work in the region very close (less than 50 nm) to the sample surface, accessing the most critical information of the optical near fields, as the signature of the optical near field is its fast decay within the range of tens of nanometers at visible and near-IR wavelengths. An alternative method for producing 3D images is to scan the sample at a constant height, and then construct 3D image by results obtained at different heights. However, scanning in a two-dimensional plane requires disabling the feedback loop, and the long measurement time can cause system drift, resulting in poor resolution in the Z direction. In the force volume method adopted here, each line curve in the Z direction is taken in less than one second, thus, the tip-sample distance is more accurately controlled. In addition, the capability of s-SNOM for mapping both amplitude and phase information make it possible to reconstruct the full three-dimensional complex field. Generally the s-SNOM tip responses much weaker to the in-plane optical field component (E_x and E_y) than to the out-of-plane component (E_z) [17] due to the optical antenna effect. With a specially designed tip, it is possible to obtain information of both the in-plane and out-of-plane components [15]. In this work, however we focus on obtaining the out-of-plane component as a demonstration of our method.

The experimental setup is a home-made transmission type s-SNOM system, which has been described in details previously [17,18]. Briefly, the system is based on a commercial AFM (CombiScope 1000, AIST-NT Inc.), and is operated in the tapping mode, with the tip oscillating at its fundamental frequency. A 633 nm HeNe laser is used as the excitation source to illuminate the measured structures from bottom. The optical field produced by the structures is scattered by the s-SNOM tip and collected in the far field with an avalanche photodiode (APD). The pseudo-heterodyne interferometry method [19] is applied to extract the near field information and to obtain both the optical amplitude and phase. The reference light required by the interferometry method is added to the light path before the APD detector to interfere with the tip scattered light. The reference light is modulated in phase to propagate the detected signal to sidebands of the harmonics of the tip oscillation frequency. A lock-in amplifier (HF2LI-MOD, Zurich Instruments) is used to perform demodulation and feed the results to the AFM collection channels. Commercial silicon tips (ARROW-NCR, Nano World) with nominal radius of 10 nm are used for the measurements in this work.

For three-dimensional measurements, an approach curve is firstly performed at each XY position of the sample surface. By raster scanning the sample, a two-dimensional array of approach curves is obtained (Fig. 1(a)). These curves form a bundle of wires, from which the volumetric information can be retrieved. For each approach curve, signals from several selected channels can be recorded simultaneously, including optical signals from sidebands of harmonic of tip oscillation frequency, the amplitude and phase of tip oscillation, and the movement of piezo stage in the Z direction. The position of each XY location, together with other operating conditions is also stored together with each approach curve file. The collected data can be the processed by numeric computation software such as MATLAB (MathWorks Inc.). The final data represent the optical near field at each voxel inside the measured volume.
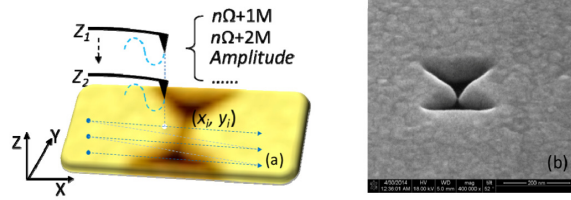
Fig. 1. (a) An illustration of the scanning process. (b) SEM images of fabricated bowtie aperture taken at an angle of 52 degrees from the side.

The sample used in this study is a bowtie aperture in 60 nm thick gold film on a glass substrate. The bowtie aperture is fabricated with focused ion beam (FEI Nova 200 dual-beam FIB). The designed dimension has an outline of 150 nm with a designed gap size around 20 nm. The SEM image of the sample is shown in Fig. 1(b). The effect of the undesired taper of the side walls will be discussed in section 4.

3. Results

Scan with the lateral size of 500 nm by 300 nm and 50 pixels by 30 pixels is performed. The free oscillation amplitude is set at 29 nm. For each approach curve in the Z direction, the sample piezo stage is swept from 100 nm to −5 nm (relative to the zero position defined by the set point, which is set at 0.8), during which 105 data points are collected. At each voxel of the measured three-dimensional space, the signals collected from different channels provide the optical amplitude and phase at that location. Since the s-SNOM tip is oscillating with its mean position at a fixed height during the process, the Z position in each approach curve is the relative position of the sample piezo stage. To better represent the 3D near field signals obtained from s-SNOM measurements, the concept of the nearest tip-sample distance is used, which means the distance between the lowest position of the tip oscillation cycle and the sample surface [20]. The Z position where the optical signal is measured can be converted to the nearest tip-sample distance with the help of simultaneously obtained tip oscillation amplitude and phase curves [20,21]. As an example, Figs. 2(a) and 2(b) show the measured tip oscillation amplitude (A_t) and phase (black curves) during tip approach process. The zero height, when the lowest position during tip oscillation is touching the sample surface, is found at the position where the tip-sample interaction just becomes net repulsive. It is the same position (Z_o) where the phase changes to below 90 degrees during approach (marked by the arrow in Fig. 2(b)). Thus the nearest tip-sample distance (D) can be calculated as $D = Z - Z_o - (A_t - A_o)$, where A_o is the tip oscillation amplitude at position Z_o. Based on this relation, the nearest distance (red curves in Fig. 2) are produced.
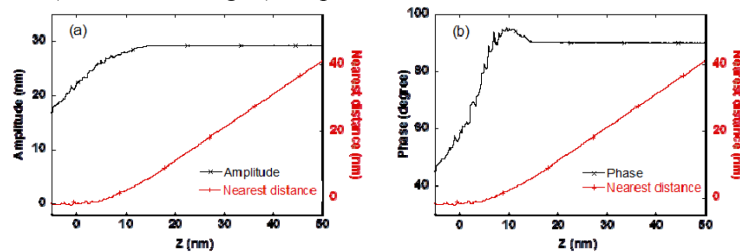

Fig. 2. The tip oscillation amplitude approach curve with the nearest tip-sample distance (a) and the tip oscillation phase approach curve with the nearest tip sample distance (b).

The nearest tip-sample distances are relative distances to each point on the sample surface. Since the surface topography is not a flat plane, it is easier to visualize the near field in vertical planes by converting the D values to the height values (Z) based on the topography of the bowtie aperture. Applying this methodology, Fig. 3 shows the amplitude and phase of the E_z field in XZ plane right across the bowtie aperture gap. In the figures, the optical field distribution is linked to the cross section profile of the bowtie aperture (the black region) i.e.,

plotted on top of the measured topography. Figure 3(a) shows the optical amplitude distribution in the space above the sample surface. The E_z field concentrates near the edges of the bowtie aperture gap as expected [17,22,23]. The strong field tightly bounds to the surface and decays fast away from the surface within a distance of about 10 nm. Because of the curvatures of the side walls of the bowtie aperture gap, the optical field exists near the gap but also spreads along the curvatures, reducing their spatial confinement. It is also noticed the field at the bottom of the gap is much weaker than the field at the top, while it should be stronger due to the narrower gap size. This is because the finite size of the SNOM tip prevents it from reaching the gap of the aperture completely, resulting a reduction in the measured signal strength. In the optical phase image (Fig. 3(b)), the characteristic 180° phase shift [17] is clearly revealed. The optical amplitude and phase in XY plane right on top of the sample surface (Z = 0) are also constructed from the volume data and shown in Figs. 3(c) and 3(d). In Fig. 3(c), two separate hot spots of the E_z field with FWHMs of about 90 nm are clearly identified, consistent with the theoretical prediction, whereas in between the two hot spots is the minimal field corresponding to the gap of the bowtie aperture [17]. The 180° phase difference between the two spots is also shown in Fig. 3(d). The figure also shows that the two hot spots are quite apart from each other with a distance of more than 100 nm. This separation is due to the gap curvatures in the fabricated bowtie aperture, which is also seen in Fig. 3(a). To illustrate the three-dimensional field, Fig. 3(e) shows the intersection of the measured XY, XZ and YZ data planes, with the YZ plane chosen at one of the hot spots. The results illustrate the fundamental resonance mode of the bowtie aperture. It is worth noting that this method is readily extended to map magnetic fields in complementary structures based on the Babinet's principle [24].
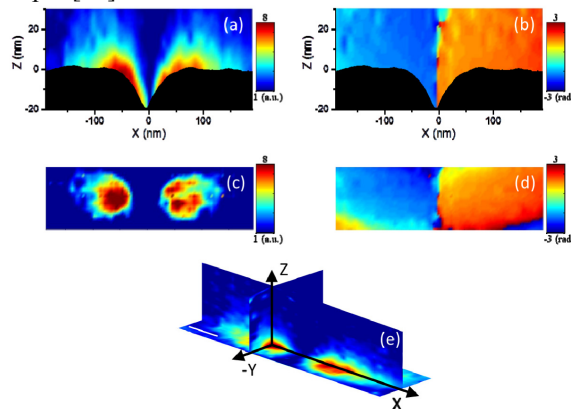

Fig. 3. The optical amplitude (a) and phase (b) images in XZ plane across bowtie aperture. The optical amplitude (c) and phase (d) images in XY plane at Z = 0. The sizes of (c) and (d) are 400 nm × 100 nm. The white scale bar in (e) is 50 nm.

4. Discussions

To examine the measured s-SNOM data, numerical simulations were performed using the commercial FEM software (HFSS, Ansoft LLC). In addition to the designed dimensions, the simulation also took into considerations of the critical curvatures obtained through the AFM topography and SEM images. The bowtie dimension at the bottom surface of the gold film is around 155 nm. Considering the curvatures to the inner wall and the edges, the dimension at the top surface of the gold film is around 220 nm. For the aperture gap, the dimensions are 9 nm at bottom, 35 nm in mid-plane, and 105 nm at the top. A top view of the modeled bowtie structure is shown in Fig. 4(a). Figure 4(b) shows the E_z field in the XY plane at the sample surface. It is found that the tapering causes not only a reduction in the field strength at the top surface, but also enlarges hot spots compared with a bowtie aperture with straight walls [17]. The amplitude and phase of the E_z field above the sample surface in the XZ plane are presented in Figs. 4(c) and 4(d), respectively. Similar behaviors of enhanced field and phase

relation between the hot spots are found comparing the calculated results and the experimental data shown in Fig. 3.
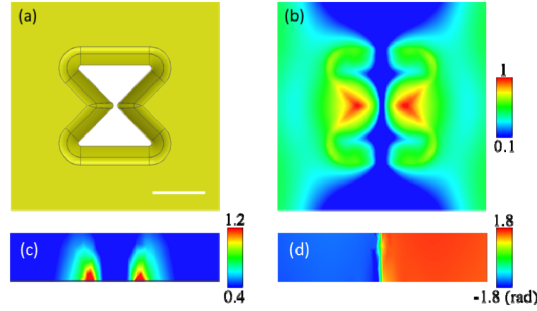

Fig. 4. (a) The simulation model of the bowtie aperture and (b) the calculated optical E_z field in the XY plane. The simulated (c) amplitude and (d) phase of E_z above the top surface of the bowtie in the XZ plane. Scale bar in (a): 100 nm. The sizes of (c) and (d) are 400 nm × 30 nm.

To further illustrate the Z dependence of the optical signals, line plots in the vertical direction are presented in Fig. 5. The plots are generated by a single vertical line going through the peak amplitude in the XZ plane. The experiment data covers a range up to 20 nm in the Z direction, while data up to 40 nm has been calculated from the simulation. It is seen from Fig. 5 that the measurements show a closely matched decay rate as the simulation result. It is noticed that the measurement data in Fig. 5 shows large field variations within a vertical distance of 10 nm or so. Meanwhile, Fig. 3(a) shows distinctive field distribution at interval of 1 nm in Z direction. These indicate a resolution of a few nanometers of the s-SNOM measurement in the Z direction. The reason for achieving such a high resolution is due to the strong dipole interaction between the tip and sample, which has also been reported in literature [25].
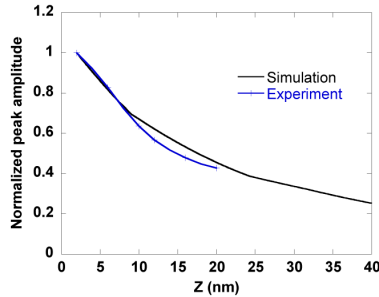

Fig. 5. The measured and calculated optical field curves in the Z direction.

5. Conclusions

In this work, s-SNOM has been applied to obtain three-dimensional optical near field information. By applying the force volume method, the accuracy in tip height position has been greatly improved. It is shown that the resolution in the Z direction of the order of a few nanometers is achieved. By comparing the measured and the simulated results, it was found that our measurement method can capture the near fields produced by a bowtie aperture. This method has the potentials in the characterization of three-dimensional field with high precision.

Acknowledgments